REPORT DOCUMENTATION PAGE

Form Approved OMB NO. 0704-0188

1. REPORT DATE (DD-MM-YYYY)	2. REPORT TYPE	3. DATES COVERED (From - To)
22-10-2008	Final Report	1-Oct-2006 - 31-Mar-2009

4. TITLE AND SUBTITLE

Final Report for Project 49449-EG, "Atomistic-Based Mesoscopic Constitutive Models for High Explosive Constituent Materials"

5a. CONTRACT NUMBER

5b. GRANT NUMBER

5c. PROGRAM ELEMENT NUMBER

611102

6. AUTHORS

Thomas D. Sewell

5d. PROJECT NUMBER

5e. TASK NUMBER

5f. WORK UNIT NUMBER

7. PERFORMING ORGANIZATION NAMES AND ADDRESSES

U.S. Energy Research and Development Adminis
Po.O. Box 5400

Albuquerque, NM 87184 -5400

8. PERFORMING ORGANIZATION REPORT NUMBER

9. SPONSORING/MONITORING AGENCY NAME(S) AND ADDRESS(ES)

U.S. Army Research Office
P.O. Box 12211
Research Triangle Park, NC 27709-2211

10. SPONSOR/MONITOR'S ACRONYM(S)

ARO

11. SPONSOR/MONITOR'S REPORT NUMBER(S)

49449-EG.1

12. DISTRIBUTION AVAILIBILITY STATEMENT

Approved for Public Release; Distribution Unlimited

13. SUPPLEMENTARY NOTES

The views, opinions and/or findings contained in this report are those of the author(s) and should not contrued as an official Department of the Army position, policy or decision, unless so designated by other documentation.

14. ABSTRACT

Large-scale molecular dynamics (MD) simulations of shocks in oriented single crystals of RDX and PETN were used to study the fundamental mechanisms by which inelastic deformation occurs when those materials are shocked to states on the Hugoniot locus modestly above the elastic limit. The goal is to identify, characterize, and quantify the dominant processes leading to localization of energy, and to capture within a statistical framework useful information concerning the local thermodynamic states behind a shock that can aid the development of improved mesoscale constitutive models. Among the homogeneously nucleated defect structures that were observed are dislocations, stacking faults, and shear bands. A method,

15. SUBJECT TERMS

Energetic Materials, Shock Waves, Molecular Dynamics, RDX, PETN, Probability Distribution Functions, Energy Localization, Plasticity

16. SECURITY CLASSIFICATION OF:			17. LIMITATION OF ABSTRACT	15. NUMBER OF PAGES	19a. NAME OF RESPONSIBLE PERSON
a. REPORT	b. ABSTRACT	c. THIS PAGE			Thomas Sewell
U	U	U	SAR		19b. TELEPHONE NUMBER: 505-667-8205

Report Title

Final Report for Project 49449-EG, "Atomistic-Based Mesoscopic Constitutive Models for High Explosive Constituent Materials"

ABSTRACT

Large-scale molecular dynamics (MD) simulations of shocks in oriented single crystals of RDX and PETN were used to study the fundamental mechanisms by which inelastic deformation occurs when those materials are shocked to states on the Hugoniot locus modestly above the elastic limit. The goal is to identify, characterize, and quantify the dominant processes leading to localization of energy, and to capture within a statistical framework useful information concerning the local thermodynamic states behind a shock that can aid the development of improved mesoscale constitutive models. Among the homogeneously nucleated defect structures that were observed are dislocations, stacking faults, and shear bands. A method, developed in collaboration with Professor D. L. Thompson at the University of Missouri-Columbia, that enables study of shocked material for times far in excess of the shock transit time across a MD simulation cell was used to study long-time relaxation phenomena in some cases. Probability distribution functions of temperature in RDX crystal were determined for slices of material perpendicular to the shock propagation direction as a function of distance in a reference frame that is stationary relative to the moving shock front.

List of papers submitted or published that acknowledge ARO support during this reporting period. List the papers, including journal references, in the following categories:

(a) Papers published in peer-reviewed journals (N/A for none)

Shock-induced shear bands in an energetic molecular crystal: Application of shock front absorbing boundary conditions to molecular dynamics simulations, Marc J. Cawkwell, Thomas D. Sewell, Lianqing Zheng, and Donald L. Thompson, Phys. Rev. B v78, 014107 (2008).

Molecular dynamics simulations of shock waves using the absorbing boundary condition: a case study of methane, Alexey V. Bolesta, Lianqing Zheng, Donald L. Thompson, and Thomas D. Sewell, Physical Review B v76, 224108 (2007).

Number of Papers published in peer-reviewed journals: 2.00

(b) Papers published in non-peer-reviewed journals or in conference proceedings (N/A for none)

Number of Papers published in non peer-reviewed journals: 0.00

(c) Presentations

Only presentations by T. D. Sewell are included.

Keynote - 8th World Congress of Computational Mechanics and 5th European Congress on Computational Methods in Applied Sciences and Engineering (Venice, Italy, June 2008).

Invited - Shock Waves in Condensed Matter (Lisbon, Portugal, May 2008).

Contributed - Shock Waves in Condensed Matter (Lisbon, Portugal, May 2008).

Keynote - Plasticity 2008 (Big Island, HI, January 2008).

Invited - APS Topical Conference on Shock Compression in Condensed Matter (Koahala Coast, Hawaii, June 2007).

Keynote - ASME Conference on Applied Mechanics and Materials (Austin, June 2007).

Number of Presentations: 6.00

Non Peer-Reviewed Conference Proceeding publications (other than abstracts):

Number of Non Peer-Reviewed Conference Proceeding publications (other than abstracts): 0

Peer-Reviewed Conference Proceeding publications (other than abstracts):

Number of Peer-Reviewed Conference Proceeding publications (other than abstracts): 0

(d) Manuscripts

Shock-induced anomalous plastic hardening in an energetic molecular crystal, Marc J. Cawkwell, Thomas D. Sewell, Kyle A. Ramos, and Daniel E. Hooks (Physical Review B, submitted).

Number of Manuscripts: 1.00

Number of Inventions:

Graduate Students

NAME	PERCENT_SUPPORTED
FTE Equivalent:	
Total Number:	

Names of Post Doctorates

NAME	PERCENT_SUPPORTED
Amy Bauer	0.75
FTE Equivalent:	**0.75**
Total Number:	**1**

Names of Faculty Supported

NAME	PERCENT_SUPPORTED
FTE Equivalent:	
Total Number:	

Names of Under Graduate students supported

NAME	PERCENT_SUPPORTED
FTE Equivalent:	
Total Number:	

Student Metrics

This section only applies to graduating undergraduates supported by this agreement in this reporting period

The number of undergraduates funded by this agreement who graduated during this period:	0.00
The number of undergraduates funded by this agreement who graduated during this period with a degree in science, mathematics, engineering, or technology fields:.....	0.00
The number of undergraduates funded by your agreement who graduated during this period and will continue to pursue a graduate or Ph.D. degree in science, mathematics, engineering, or technology fields:.....	0.00
Number of graduating undergraduates who achieved a 3.5 GPA to 4.0 (4.0 max scale):	0.00
Number of graduating undergraduates funded by a DoD funded Center of Excellence grant for Education, Research and Engineering:	0.00
The number of undergraduates funded by your agreement who graduated during this period and intend to work for the Department of Defense	0.00
The number of undergraduates funded by your agreement who graduated during this period and will receive scholarships or fellowships for further studies in science, mathematics, engineering or technology fields:	0.00

Names of Personnel receiving masters degrees

NAME
Total Number:

Names of personnel receiving PHDs

NAME
Total Number:

Names of other research staff

NAME	PERCENT_SUPPORTED	
Thomas D. Sewell	0.03	No
FTE Equivalent:	**0.03**	
Total Number:	**1**	

Sub Contractors (DD882)

Inventions (DD882)

FINAL REPORT FOR PROJECT 49449-EG, "ATOMISTIC-BASED MESOSCOPIC CONSTITUTIVE MODELS FOR HIGH EXPLOSIVE CONSTITUENT MATERIALS"

FOREWORD

This Final Report pertains to work performed by Thomas D. Sewell and postdoctoral co-workers Marc J. Cawkwell and Amy L. Bauer at Los Alamos National Laboratory and the Donald L. Thompson Group in the Department of Chemistry at the University of Missouri-Columbia during the time period 10/06-8/08 under the auspices of ARO project 49449-EG. The project was terminated upon the departure of Sewell from the Theoretical Division at Los Alamos in August 2008 to accept a faculty position in the Department of Chemistry at the University of Missouri-Columbia.

LIST OF ILLUSTRATIONS

prevent reflected waves from propagating back into the cell. (See Refs. 2 and 3 for details.)

Figure 7: Snapshots from simulation of homogeneously nucleated shear bands in RDX crystal shocked along [100]. (a) system at the moment the shock wave reaches the right-hand end of the simulation cell, at which point the shock front absorbing boundary condition was applied; (b) system at a time 100 ps after application of the shock front absorbing boundary condition. CR and SB denote regions of material from crystalline regions and shear band regions, respectively, that were used for subsequent detailed analysis.

Figure 8: Temperature versus time for (100)-oriented RDX crystal shocked to P=9.7 GPa. Results are shown for material in a shear band and for material in a crystalline region. Both intramolecular (vibrational) and intermolecular temperatures are shown.

Figure 9: Two-dimensional map of temperature behind a 9.7 GPa shock in (100)-oriented RDX crystal. Color bar units in Kelvin. The shock front has passed from left to right through the material. Defect structures evident in the temperature map are homogeneously nucleated shear bands. Arrows indicate distances of 5 nm and 140 nm behind the shock front. The original simulation cell was ~0.18 x 0.18 x 0.005 micron.

Figure 10: Normalized probability distribution functions (PDFs) for temperature in (100)-oriented RDX crystal shocked to 9.7 GPa. Results are shown for thin slices of material perpendicular to the direction of shock propagation, for several distances (or, equivalently, times) behind the shock front. Top: PDFs for six distances ranging from 5 nm to 160 nm behind the shock front (dark blue to yellow, respectively) based on the analysis of a single simulation snapshot corresponding to t = 36 ps. Bottom: as above, but with axes rotated and averaging over all equivalent time origins in a frame centered on the moving shock front.

Figure 11: Profiles of intermolecular and intramolecular temperature as functions of distance behind the shock front for shock waves with U_p = 1 km/s propagating along the [100], [111], and [210] directions in RDX crystal.

Figure 12: Preliminary result from an in-progress simulation of shock wave propagation along [100] in single-crystal PETN. The piston velocity is U_p = 1 km/s. The shock front is midway through the crystal; nucleation of plasticity at distances significantly behind the shock front is evident.

STATEMENT OF THE PROBLEMS STUDIED

The main goal of this project was to obtain on the basis of the analysis of large-scale unreactive molecular dynamics

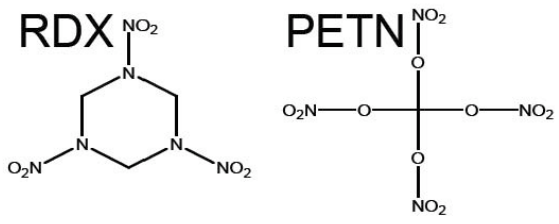

Figure 1. Chemical structures of hexahydro-1,3,5-trinitro-1,3,5-triazine (RDX), and pentaerythritol tetranitrate (PETN).

(MD) simulations a molecular-level understanding of plasticity and relaxation mechanisms in polyatomic molecular systems, and to use this information to guide the formulation of mesoscopic constitutive models for the constituents of energetic materials formulations. The principal focus was on the cyclic nitramine hexahydro-1,3,5-trinitro-1,3,5-triazine (RDX); studies of the nitrate ester pentaerythritol tetranitrate (PETN) were also undertaken near the end of the project. (See Fig. 1 for sketches of the RDX and PETN molecular structures.) The focus was on shock wave loading to states above, but fairly close to, the Hugoniot elastic limit for oriented crystals of material without any pre-existing defects; preliminary studies were performed for the case of RDX crystals containing cylindrical voids in a quasi 2-D simulation cell. (Figure 2 contains a depiction of the way in which shock waves were generated in these studies.[1])

Our approach to the problem included three principal components:

- Identify, for shock propagation along a given direction in a given crystal, the dominant mechanism(s) of inelastic deformation for shock loading to a given state on the Hugoniot locus.
- Characterize these mechanisms and the resulting energy localization in terms of molecular-scale phenomena by using descriptors that capture both the "standard" translational degrees of freedom associated with inelastic deformation in metals as well as additional ones specific to molecular entities that are required as a consequence of their non-spherical shapes, intramolecular flexibility, and in some cases point-group polymorphism or even chemical transformation.
- Quantify the practical outcomes of these inelastic deformation processes on mesoscopic distributions of thermodynamic variables (temperature, stress) through the use of probability distribution functions that capture the evolution of those variables, and correlations between those variables, as functions of distance or, equivalently, time after shock passage.

During the course of the research we discovered that these complicated materials deform *via* pathways that are in some ways similar to those for metals. For example, we observed the formation of dislocations, stacking faults, and shear bands depending on which material was studied and the direction and intensity of shock loading. However, we also confirmed our expectation that the observed behaviors include, and in some cases are dominated by, features for which there are no analogues in metals. An additional complication that had to be addressed during this work was the long time scale, relative to the shock wave transit time across a molecular dynamics simulation cell, required for relaxation of homogeneously nucleated defects that developed under certain loading conditions. An approach to dealing with this problem was conceived by Prof. D. L. Thompson at The University of Missouri-Columbia (MU) during the time frame of this project; a collaborative effort between

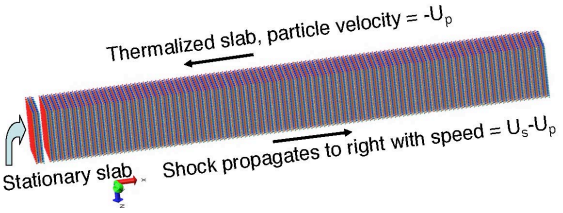

Figure 2. Method used to generate shock waves. Three-dimensional periodic boundary conditions were used, with a several hundred-Ångstrom gap introduced at one end of the "long" dimension so that the stationary slab on the left-hand end and the free surface on the right-hand end of the periodic simulation cell do not interact. The color scheme is only intended as an aid for the eye.

MU and LANL resulted in an initial method development paper followed by an application directly related to the present project.[2,3] Finally, probability distribution functions were constructed that capture, on the basis of analyses of simulations containing ~500,000 fully flexible molecules, the evolution of temperature in RDX as a function of distance behind the shock front in that material. This kind of information, and in particular the evolution of the high temperature tails of the distribution corresponding to extreme fluctuations in the material, are important to the development of advanced mesoscale models of energetic materials initiation under development by Mel Baer[4,5] at Sandia National Laboratory and Jack Reaugh[6] at Lawrence Livermore, among others.

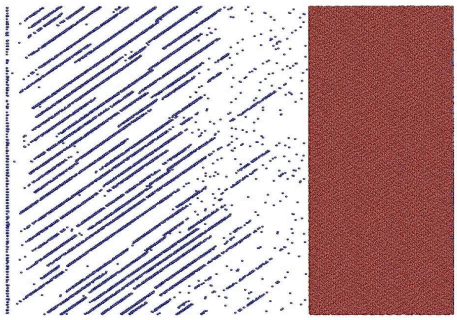

Figure 3. Development of stacking faults for RDX shocked at U_p = 300 m/s along the [111] direction. Only the centers of mass of molecules that have changed numbers of nearest neighbors relative to the nominal equilibrium structure are shown. The original simulation cell dimensions were approximately 0.18 x 0.18 x 0.005 micron.

SUMMARY OF THE MOST IMPORTANT RESULTS

Simulation and characterization of homogeneous nucleation of stacking faults in (111)-oriented RDX. Simulations of shock loading along the [111] direction in RDX revealed an abrupt onset of homogeneous nucleation of partial dislocation loops on (001) with Burgers vector 0.16[010]. (See Fig. 3.) The onset occurs for shock pressures 1.37 GPa < $P_{RH} \leq$ 1.78 GPa. The partial dislocation loops generate stacking faults that are obstacles for the glide of perfect dislocations on other slip systems, giving rise to an anomalous hardening that does not involve the mutual entanglement and storage of dislocations. Calculations of the [010] cross-section of the (001) generalized stacking fault energy surface as a function of applied pressure show that this stacking fault is rendered metastable by a stress-induced change in the molecular conformation. Anomalous hardening *via* this mechanism is predicted to result in high impact sensitivity, in apparent contrast to the conclusion one would obtain upon application of Dick's[7] steric hindrance model using slip systems determined from indentation experiments. The results of this paper demonstrate:[8]

- the importance of including the resolved stress on the stacking fault plane in order to render the stacking fault metastable; this effect apparently is unimportant for metals, due to the lack in that case of internal degrees of freedom (flexibility) and non-spherical particle shapes (atoms versus polyatomic molecules). (See Fig. 4.)
- the need for careful thermalization at each displacement along the Burgers vector when computing the generalized γ-surface *enthalpy* profile, to relax those intramolecular and intermolecular interactions; in particular, molecules in the neighborhood of the stacking fault undergo changes in molecular conformation and orientation in the crystal (see Fig. 5).
- the need to exercise care when applying the steric hindrance model to predict initiation sensitivity; in particular, to assess the slip systems that are actually

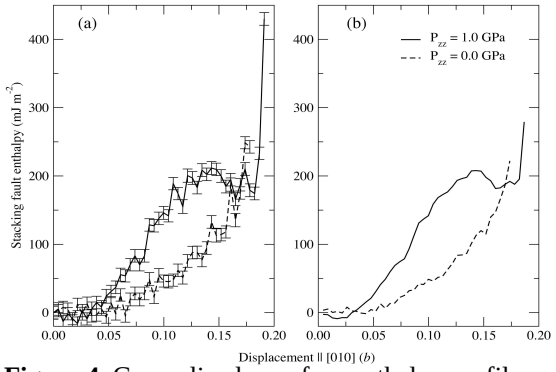

Figure 4. Generalized γ-surface enthalpy profiles for the cases P_{zz} = 0 GPa and P_{zz} = 1 GPa along the Burgers vector determined for stacking faults generated by shock waves propagating along [111] in RDX. Left: plots including estimates of precision. Right: same, but with error bars removed for ease of interpretation. It is necessary to include the component of stress normal to the stacking fault plane in order to render the stacking fault metastable.

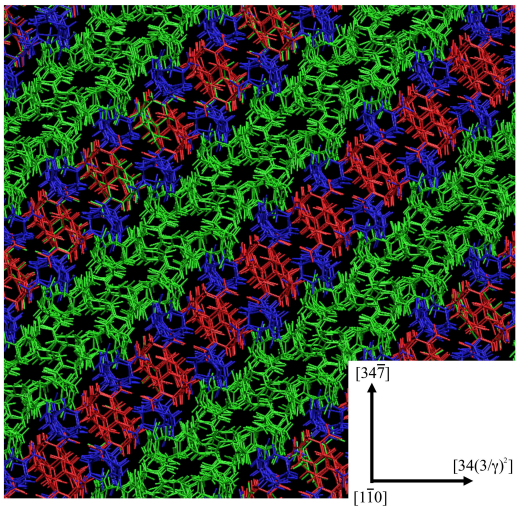

Figure 5. All-atom view of stacking faults in (111)-oriented RDX. $\gamma=c/a$ (lattice lengths).

operative under the regime of strain rates of interest rather than extrapolating across orders of magnitude from static indentation to shock. [PETN appears to be something of a "pathological" case in this regard, possibly due to its small unit cell (two molecules) and relatively high space group symmetry.]

Extension of the Shock Front Absorbing Boundary Condition and study of homogeneously nucleated shear bands in shocked (100)-oriented RDX single crystal. The response of the energetic molecular crystal RDX to the propagation of planar shock waves normal to (100) was also studied.[3] In this case, we observed the nucleation and spread of shear bands during shocks with a particle velocity of 1.0 km/s and corresponding Rankine-Hugoniot shock pressure of 9.7 GPa. These defects propagate into the compressed material at 45° to [100] in the (010) zone, and lead to localized temperature rise due to viscous heating in the shear bands. In contrast to the case discussed above, however, the shear bands evolve slowly compared to the time scales required for the shock wave to traverse the simulation cell. Thus, a recently developed[2] shock front absorbing boundary condition was applied (Fig. 6), with some adaptation, to the simulation cells studied here to sustain the shock-compressed state.[3] This enabled simulations of sufficient duration to study the temporal and structural evolution of the shock-induced shear bands toward a steady-fluctuating state. Analyses of orientational and conformational disorder were performed and contrasted for regions within and external to the shear bands (Fig. 7). Additionally, an estimate of the "shock underheating" due to the classical approximation was performed. The major

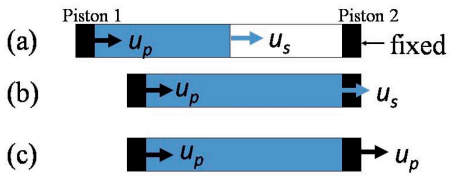

Figure 6. Schematic depiction of the shock front absorbing boundary condition approach used to the sustain the initial volume/energy shock state for times beyond that required for shock wave traversal of the MD simulation cell. The essence of the method is to capture between two rigid pistons the state of the material at the instant in time that the shock wave reaches the "free surface" of a normal non-equilibrium simulation cell, to prevent reflected waves from propagating back into the cell. (See Refs. 2 and 3 for details.)

conclusions from this work are:

- Due to intense viscous heating within them, the shear bands can be considered to be homogeneously nucleated hot spots (Fig. 8).
- Two of the three structural determinants that characterize liquid behavior -- molecular reorientation/conformational relaxation and pair distribution function g(r) -- were studied and confirmed that material in the shear band is indeed liquidlike; the third, self-diffusion, was not considered due to the complicated counterflow boundary conditions associated with the shear bands.
- Both molecular orientations and intramolecular properties (distributions of axial and equatorial NO_2 groups and boat/chair/half-boat six-member ring conformations) are sensitive indicators of shear banding.
- For the 9.7 GPa shock strength considered here, the time constant for rotational reorientation in the shear band is ~15 ps.

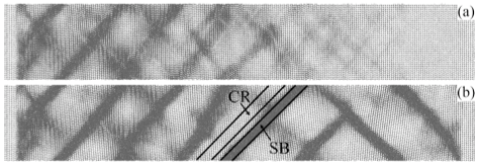

Figure 7. Snapshots from simulation of homogeneously nucleated shear bands in RDX crystal shocked along [100]. (a) system at the moment the shock wave reaches the right-hand end of the simulation cell, at which point the shock front absorbing boundary condition was applied; (b) system at a time 100 ps after application of the shock front absorbing boundary condition. CR and SB denote regions of material from crystalline regions and shear band regions, respectively, that were used for subsequent detailed analysis.

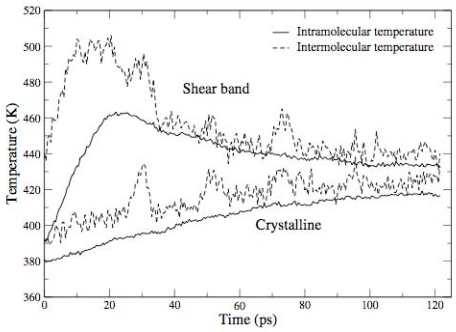

Figure 8. Temperature versus time for (100)-oriented RDX crystal shocked to P=9.7 GPa. Results are shown for material in a shear band and for material in a crystalline region. Both intramolecular (vibrational) and intermolecular temperatures are shown.

- Using the shock front absorbing boundary condition, it was practical to simulate a system for times sufficiently long to observe nucleation, growth, and eventual quenching and cooling (*via* thermal conduction) of the shear bands.
- A careful analysis based on equation of state considerations was performed to estimate the magnitude of underheating compared to experiment for the simulated shock in regions far-removed from shear bands. The underheating arises due to differences in behavior of the classical mechanical and quantum mechanical specific heat of the material, the former corresponding to the molecular dynamics simulations and the latter to the real material.

Probability distribution functions of temperature in RDX crystal shocked along [100]. The average temperatures attained by purely hydrodynamic shock heating are insufficient to initiate significant chemical reactions in plastic-bonded explosives, even for bulk shock pressures for which detonation initiation is known to occur. Thus, energy localization processes, whether homogeneously or heterogeneously nucleated, are required to achieve sufficiently high local energy density ("hot spots") for rapid chemistry to initiate (Fig. 9). Moreover, given the exponential dependence of chemical reaction rates with temperature, it is the extreme fluctuations in local temperature,

corresponding to the high-temperature tails of the associated distribution functions, which will dominate the earliest stages of initiation chemistry. (Analogous comments apply to the importance of local stress in the shocked material.)

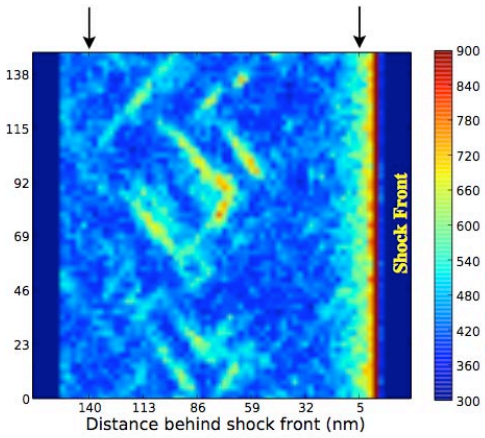

Figure 9. Two-dimensional map of temperature behind a 9.7 GPa shock in (100)-oriented RDX crystal. Color bar units in Kelvin. The shock front has passed from left to right through the material. Defect structures evident in the temperature map are homogeneously nucleated shear bands. Arrows indicate distances of 5 nm and 140 nm behind the shock front. The original simulation cell was ~0.18 x 0.18 x 0.005 micron.

In order to characterize these temperature fluctuations, real space probability distribution functions of temperature in (100)-oriented RDX crystal shocked to P = 9.7 GPa (sufficient to nucleate shear banding in the material; see preceding section) were determined as a function of distance or, equivalently, time after shock passage through the material (Fig. 10, top panel). Thus, each of the six curves in top panel of Fig. 10 corresponds to the distribution of temperatures observed in a slice of material perpendicular to the direction of shock propagation, at distances ranging from 5 nm to 160 nm behind the shock front. Even though each of these distribution functions is based on the kinetic energies of several thousand molecules, the statistics are rather noisy. However, by choosing a reference frame that is stationary with respect to the moving shock front, it is possible to collect simulation data over multiple time origins and therefore improve significantly the accuracy and precision of the distributions (Fig. 10, bottom panel). These improved statistics bring into relief the rapid relaxation, within tens of nm behind the shock front in the present case, of an initial tail in the temperature distribution distances that extends out to ~1000 K, even though the average temperature behind the shock wave is only ~400 K.

The results shown here are limited to single variable (temperature) probability distribution functions (PDFs) for slices of material perpendicular to the direction of shock propagation and at specific distances behind the shock front. While this kind of information is interesting, access to conditional PDFs will yield considerably more information of use to mesoscale model development. For example, determining the conditional PDF for observing a temperature T at some point y given a temperature T' at some point y', both at some distance x behind the shock front, will begin to provide information concerning spatial correlations among hot regions in the material; extension to time evolution of these spatial correlations (by interpolating between slices corresponding to different distances behind the shock) should be straightforward, and will lead to tangible information concerning three-dimensional hot spot sizes and shapes. Probability distribution functions analogous to those described above, but for which stress is the variable of interest, as well as multivariate PDFs involving both temperature and stress (and possibly local strain or strain deformation gradient), are also of significant interest. Finally, an intriguing possibility is to study these PDFs in reciprocal space, since important structures in the data may not be apparent in the real-space picture yet may

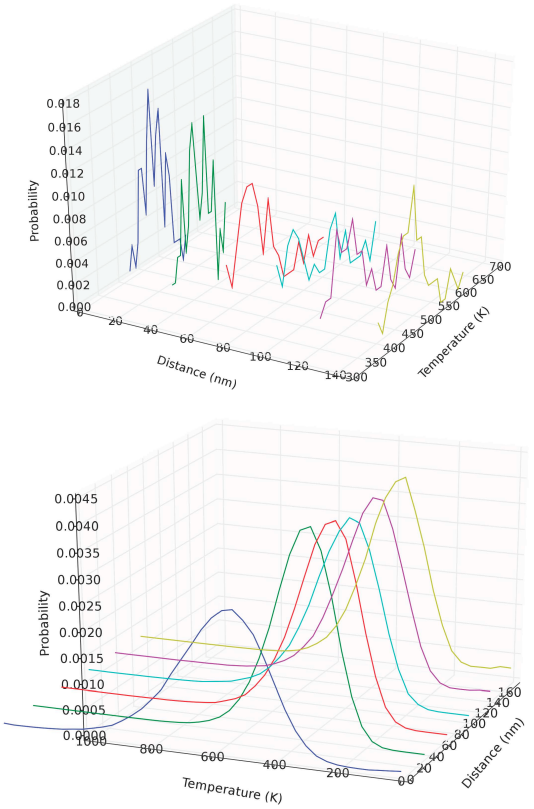

Figure 10. Normalized probability distributions (PDFs) for temperature in (100)-oriented crystal shocked to 9.7 GPa. Results are shown for thin slices of material perpendicular to the direction of shock propagation, for several distances (or, equivalently, times) behind the shock front. Top: PDFs for six distances ranging from 5 nm to 160 nm behind the shock front (dark blue to yellow, respectively) based on the analysis of a single simulation snapshot corresponding to t=36 ps. Bottom: as above, but with axes rotated and averaging over all equivalent time origins in a frame centered on the moving shock front.

stand out clearly in reciprocal space. These latter possibilities comprise a research area of intense ongoing interest.

Additional Studies. Additional studies that were begun during this contract include simulations of shock waves with U_p = 1 km/s propagating along three different directions in single crystal RDX (Fig. 11) and a simulation of PETN crystal shocked along [100] at U_p = 1 km/s (Fig. 12). In the case of the RDX simulations, plots of intermolecular and intramolecular temperature profiles as functions of distance (or, equivalently, time) behind the shock front, determined for different directions of shock wave propagation ([100], [111], and [210]) reveal significant differences in the extent of initial overheating of lattice modes (intermolecular temperature) and distances required for the approach to thermal equilibrium among the intermolecular and intramolecular measures of temperature. Understanding the origins of these differences in terms of fundamental deformation processes and dynamical energy transfer mechanisms is of keen intellectual interest, and will lead to useful insight concerning intrinsic shock initiation sensitivity.

The result shown for (100)-oriented PETN indicates the onset of plasticity. The details of the deformation have yet to be explored, however, in spite of the current interest in understanding and assessing the steric hindrance model as an explanation for anisotropic initiation sensitivity based on the presence or absence of plastic slip systems for different directions of shock loading. While neither of these investigations reached a point that warrants extensive discussion, both have revealed intriguing behaviors that should form the basis of future research.

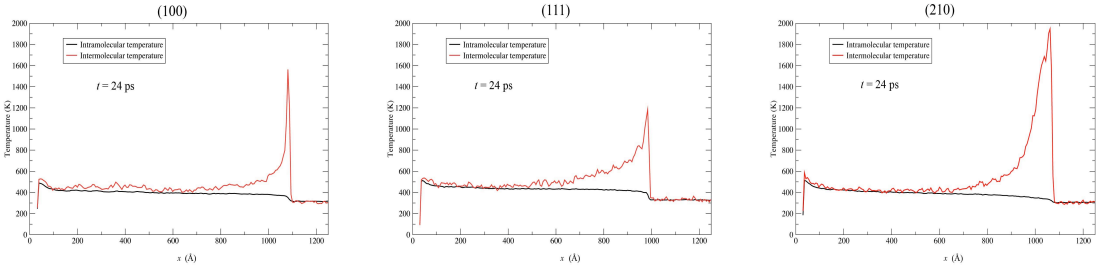

Figure 11: Profiles of intermolecular and intramolecular temperature as functions of distance behind the shock front for shock waves with U_p = 1 km/s propagating along the [100], [111], and [210] directions in RDX crystal.

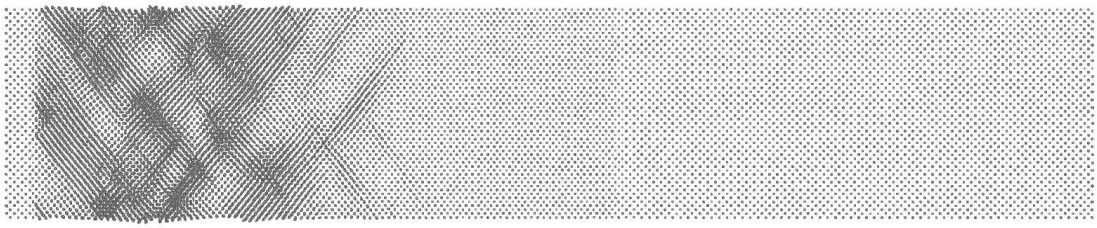

Figure 12. Preliminary result from an in-progress simulation of shock wave propagation along [100] in single-crystal PETN. The piston velocity is U_p = 1 km/s. The shock front is midway through the crystal; nucleation of plasticity at distances significantly behind the shock front is evident.

LITERATURE CITED

[1] E. Jaramillo, T. D. Sewell, and A. Strachan, *Atomic-level view of inelastic deformation in a shock loaded molecular crystal*, Phys. Rev. B **76**, 064112 (2007).
[2] A. V. Bolesta, L. Zheng, D. L. Thompson, and T. D. Sewell, *Molecular dynamics simulations of shock waves using the absorbing boundary condition: A case study of methane*, Phys. Rev. B **76**, 224108 (2007).
[3] M. J. Cawkwell, T. D. Sewell, L. Zheng, and D. L. Thompson, *Shock-induced shear bands in an energetic molecular crystal: Application of shock-front absorbing boundary conditions to molecular dynamics simulations*, Phys. Rev. B **78**, 014107 (2008).
[4] M. R. Baer and W. L. Trott, *Mesoscale descriptions of shock-loaded heterogeneous porous materials*, in Shock Compression of Condensed Matter – 2001, M. D. Furnish, N. N. Thadhani, and Y. Horie Eds. (AIP, 2002) p. 713.
[5] M. R. Baer, *Modeling heterogeneous energetic materials at the mesoscale*, Thermochimica Acta **384**, 351 (2002).
[6] J. E. Reaugh, *Grain-scale dynamics in explosives*, Lawrence Livermore National Laboratory report UCRL-ID-150388 (2002).
[7] J. J. Dick, *Anomalous shock initiation of detonation in pentaerythritol tetranitrate crystals*, J. Appl. Phys. **81**, 601 (1997).
[8] M. J. Cawkwell, T. D. Sewell, K. J. Ramos, and D. E. Hooks, *Shock-induced anomalous plastic hardening in cyclotrimethylene trinitramine (RDX)* (Phys. Rev. B, submitted).